

Research Article

Preparation and *In Vivo* Expression of CS-PEI/pCGRP Complex for Promoting Fracture Healing

Chun-Liang Li,¹ Feng Qin,² Rong-rong Li,³ Jia Zhuan,⁴ Hai-Yong Zhu,¹ Yu Wang,¹ and Kai Wang¹ 

¹Department of Orthopedics, Qinghai Provincial People's Hospital, Xining, Qinghai, China

²Department of Endocrinology, University Affiliated Hospital, Xining, Qinghai, China

³Qinghai Nationalities University, Xining, Qinghai, China

⁴Department of Clean Operation, Qinghai Provincial People's Hospital, Xining, Qinghai, China

Correspondence should be addressed to Kai Wang; wkkw002@sina.com

Received 18 October 2018; Revised 11 November 2018; Accepted 22 November 2018; Published 19 February 2019

Guest Editor: Jianxun Ding

Copyright © 2019 Chun-Liang Li et al. This is an open access article distributed under the Creative Commons Attribution License, which permits unrestricted use, distribution, and reproduction in any medium, provided the original work is properly cited.

Background/Objective. CGRP is a calcitonin gene-related peptide that is capable of promoting bone development and bone regeneration. Chitosan is a nontoxic and degradable biomaterial. However, the gene transfection efficiency of chitosan is low, whereas PEI (polyethyleneimine) has higher capability of transfection efficiency. In this paper, PEI was covalently linked to chitosan, and the rat CGRP plasmid was encapsulated in a CS-PEI complex to construct CS-PEI/pCGRP nanoparticles. The characterization and biological effects of CS-PEI/pCGRP nanoparticles were investigated *in vivo*. **Methods.** CS-PEI/pCGRP nanoparticles were prepared by a complex coacervation method. The PEI distribution degree on chitosan was measured with a dialysis method and ¹H-NMR analysis. The particle size and zeta potential of CS-PEI/pCGRP nanoparticles were detected by dynamic light scattering. The binding of CS-PEI to pCGRP was detected by gel retardation assay. The transfection effect was evaluated by RT-qPCR. A rat femoral fracture model was established and treated with PBS, pCGRP, CS-PEI, and CS-PEI/pCGRP to detect the expression of CGRP and downstream genes in early healing of fractures by RT-qPCR, western blot, and immunohistochemistry (IHC). **Results.** The particle size and zeta potential of CS-PEI/pCGRP nanoparticles were stable when the mass ratio of CS-PEI and pCGRP was higher than 5:1, the ratio which could also effectively protect pCGRP from DNase I degradation. CS-PEI/pCGRP could obviously increase CGRP expression in rat bone marrow stromal cells. *In vivo* fracture healing experiments demonstrated that CGRP could be delivered to the body via the CS-PEI and expressed *in situ* after a 3-week treatment. Moreover, CS-PEI/pCGRP significantly enhanced the mRNA and protein levels of downstream RUNX2 and ALP. **Conclusion.** CS-PEI/pCGRP nanoparticles were an effective nonviral gene transfection system that could upregulate CGRP expression *in vivo* and accelerate the expression of key biomarkers for early healing of fractures.

1. Introduction

With the increase of people's activity and space, the possibility of bone fracture rises. And the increasing number of osteoporosis patients caused by aging results in continuous increase of fracture incidence. About 50% of women and 20% of men in their lifetime will experience fragility fractures [1–4] and consequent high cost of medical care (costs associated with fragility fractures). In 2006, China spent 1.6 billion USD on hip fracture care, which is projected to rise to 12.5 billion USD by 2020 and 265 billion USD by 2050 [5]. With

the development of biomaterials, it has been the focus of bone repair research for tissue engineering biomaterials as transplant substitutes in recent years. Bone tissue engineering has made “local repair” of the fracture area and systematically enhanced bone repair ability to regenerate normal bone tissue, which has achieved considerable results.

Fracture healing is a complex physiological process accompanied by the formation of local hematoma and local inflammation. The healing process involves the proliferation, differentiation, and matrix mineralization of osteoblasts. The treatment strategies to control inflammation, promote blood

circulation, and stimulate bone regeneration can improve fracture healing. Gene therapy induces human normal genes or therapeutic genes into targeted cells in some certain ways to correct gene defects and has achieved clinical effect by induction of single or multiple genes to accelerate the fracture healing. CGRP is a calcitonin gene-related peptide, which is a neuropeptide that distributes in the active region of bone growth [6]. CGRP plays an important role in nourishing nerves and blood vessels; it also plays an anti-inflammatory role, directly promoting osteoblast proliferation, differentiation, and mineralization, thereby promoting bone development and bone regeneration [7]. For example, CGRP can induce differentiation of adipose-derived stem cells into osteoblasts and maintain high cell proliferative capacity, as well as induce exuberant secretion of extracellular matrix, and upregulate BMP2 expression which can promote osteogenic activity of osteoblasts [8]. However, there are still few studies on the role of CGRP in fracture healing, and it is beneficial to investigate how CGRP promotes bone regeneration.

Chitosan is a natural polycationic and weak alkaline polysaccharide with excellent biocompatibility and degradability [9]. It is safe and nontoxic, which is regarded as one of the most promising drug-loading materials [10]. Mumper et al. [11] first reported the use of chitosan in gene delivery *in vitro*. Many studies have shown that the physicochemical properties (size, zeta potential, and nucleic acid complexation efficiency) of chitosan/gene complex directly affect gene delivery efficiency [12, 13]. It is generally recognized that a diameter of complex, smaller than 200 nm with a positive potential [14], holds the highest transfection efficiency, so the ratio of chitosan to nucleic acid and the preparation method are the key factors affecting these physical and chemical properties [15]. Polyethyleneimine (PEI), like chitosan, is a cationic nonviral gene carrier that binds to proteoglycans on the cell surface and enters cells by endocytosis. PEI facilitates the escape of carriers from lysosomes by "proton sponge effect," thereby increasing transfection efficiency [16]. In this study, PEI with a small molecule mass was covalently grafted onto the chitosan backbone to prepare chitosan-PEI (CS-PEI) composite carrier, and CGRP plasmid (pCGRP) was packaged by CS-PEI to synthesize CS-PEI/pCGRP nanoparticles. The physical properties of CS-PEI/pCGRP nanoparticles were detected. *In vivo* gene transfection experiments were performed to study the role of CS-PEI/pCGRP complex in promoting fracture healing.

2. Method

2.1. Materials. The pCDNA3.1⁺ plasmid containing the rat CGRP sequence (pCGRP) was constructed and transformed into *E. coli* to amplify and extract the plasmid.

2.2. Preparation of CS-PEI/pCGRP Nanoparticles. In Figure 1, according to previous reports by Tripathi et al. [17], 100 mg of chitosan (85% deacetylated, Sigma) was dissolved in a 1% hydrochloric acid (HCl) solution and stirred at 60°C overnight. Afterwards, 0.25 mL of epichlorohydrin was added, stirred for 3 hours, and concentrated to a white

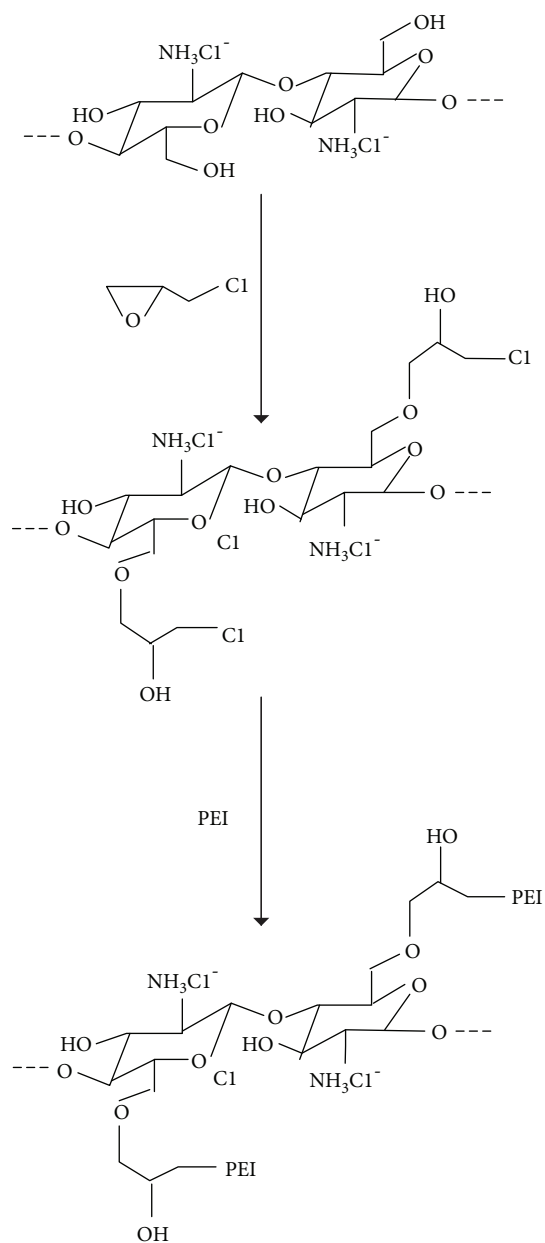


FIGURE 1: Reaction scheme of constructing CS-PEI.

powder on a rotary evaporator to achieve chitosan chlorohydrin hydrochloride (CC). CC and PEI (Sigma) with a mass ratio of 1:4 were dissolved in 100 mL of water, heated to 60°C, supplemented with NaOH solution (2 mol/L, 2 mL), and stirred at 60°C for 20 h. The resulting solution was purified with a dialysis method and lyophilized to obtain CS-PEI. The distribution degree of PEI on CS-PEI was calculated by the following equation:

$$\text{Distribution degree (\%)} = 100\% \times \frac{W_1 - W_0}{W_0}, \quad (1)$$

where W_0 is the initial weight of chitosan and W_1 is the weight of CS-PEI.

CS-PEI was dissolved in water to prepare a solution of $0.5 \mu\text{g}/\mu\text{L}$ and stirred overnight. An appropriate amount of CGRP plasmid DNA was added to the CS-PEI solution and stirred for 2 min to prepare a CS-PEI/pCGRP nanoparticle solution.

2.3. $^1\text{H-NMR}$ Characterization of CS-PEI Nanoparticles. CS and CS-PEI were dissolved in a $\text{CD}_3\text{COOD}/\text{D}_2\text{O}$ solvent, and the $^1\text{H-NMR}$ spectrum was determined using a Mercury-plus 400 NMR spectrometer (Varian, CA, USA).

2.4. Dynamic Light Scattering Detection of Particle Size and Zeta Potential. The CS-PEI/pCGRP complex containing different mass ratios (CS-PEI:) was sufficiently diluted, added to the sample cell, and placed in a nanoparticle-size analyzer (Delsa Nano C Particle Analyzer, Beckman Coulter Inc.) to measure the particle size and zeta potential of the sample.

2.5. Agarose Gel Retardation Electrophoresis Experiment. 5 U DNase I (Qiagen) was added into the CS-PEI/pCGRP complex solution containing CS-PEI and pCGRP in different mass ratios under 37°C water bath. One hour later, 25 mM EDTA was added to stop the reaction. 1% agarose gel electrophoresis was performed to analyze the binding ability of the CS-PEI carrier to plasmid, and pCGRP was used as control.

2.6. Culture of Rat Bone Marrow Stromal Cells and In Vitro Transfections by CS-PEI/pCGRP. As previously discussed [18], rat bone marrow stromal cells (BMSCs) were isolated from the femur and tibia and cultured in IMDM supplemented with 20% FBS. The adherent BMSCs were used for further assay after 3 days of culture.

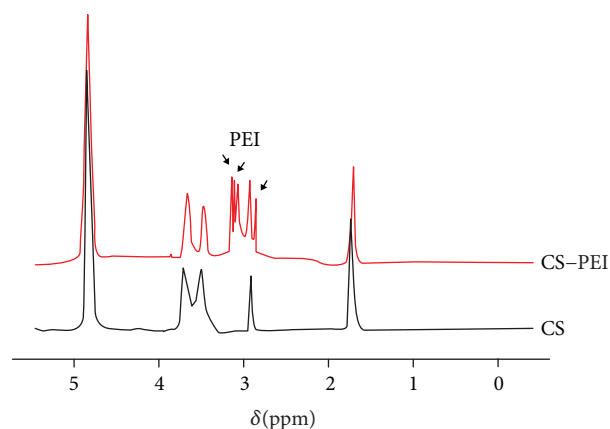
Next, cells were trypsinized, washed, centrifuged, and seeded in a 6-well plate at the density of 100,000/well. After overnight culture, the medium was replaced with a serum-free medium containing CS-PEI/pCGRP with different mass ratios of CS-PEI to pCGRP from 1:2 to 8:1. The amount of pCGRP was $2 \mu\text{g}$ in every well. After 6 hours of culture, cells were then continuously cultured for 48 h with a complete medium. Then, CGRP mRNA levels of BMSCs were evaluated by gene quantification.

2.7. Preparation of Rat Femoral Fracture Model and Interventional Treatment of CS-PEI/pCGRP. 20-month-old Sprague-Dawley male rats were provided by the Experimental Animal Center of Lanzhou University (Lanzhou, China). All rats were prepared for the right femoral fracture model. In brief, the middle part of the right hind leg was surgically exposed after anesthesia and the middle part of the femur was sawn to induce a short transverse fracture. A 1 mm diameter Kirschner wire was then threaded into the medullary cavity of the femur. The fracture was fixed and the wound was closed after surgery. The rats were intraperitoneally injected with 100,000 U of penicillin sodium daily for 3 days. Three days after the operation, 48 rats were selected under imaging without obvious displacement at the broken site and loosening at the internal fixation.

The rats were randomly divided into 4 groups: PBS control group, pCGRP treatment group, CS-PEI treatment group, and CS-PEI/pCGRP treatment group. The rats were

TABLE 1: PCR primer sequences.

Gene	Primer sequences
CGRP	F: 5'-AGCCCCAGATCTAAGCGGTGTG-3'
	R: 5'-TCCTTGGCCATATCCCTTTTCTTG-3'
ALP	F: 5'-CTCAACACCAATGTAGCCAAGAATG-3'
	R: 5'-GGCAGCGTTACTGTGGAGA-3'
RUNX2	F: 5'-GCACAAACATGGCCAGATTCA-3'
	R: 5'-AAGCCATGGTGCCCGTTAG-3'
β -Actin	F: 5'-CATCCGTAAAGACCTCTATGCCAAC-3'
	R: 5'-ATGGAGCCACCGATCCACA-3'

FIGURE 2: $^1\text{H-NMR}$ spectra of CS and CS-PEI.

fixed after anesthesia, and $250 \mu\text{L}$ of various solutions was slowly injected subcutaneously at the fracture site. The injection time was not shorter than 1 min. The amount of pCGRP was $20 \mu\text{g}$, and the mass ratio of CS-PEI:pCGRP was 8:1. For the mice in the CS-PEI treatment group, the amount of CS-PEI was equal to the amount of CS-PEI/pCGRP in the mice of the CS-PEI/pCGRP treatment group.

2.8. Immunohistochemistry (IHC) Staining to Detect the Expression of CGRP in Bone Tissue. Animals were sacrificed 3 weeks after treatment. The femur samples from four rats in each group were taken and fixed in 4% paraformaldehyde for 12 h. Decalcification (Fuyang Biotek, Shanghai, China) was performed to make $5 \mu\text{m}$ thick paraffin sections. The sections were routinely dewaxed, hydrated, washed with PBS, and incubated with 3% hydrogen peroxide for 20 min at room temperature to block endogenous peroxidase activity. After blocking with rabbit serum, the slides were incubated with CGRP primary antibody (Bioss, Beijing, China) at 4°C overnight and then incubated with secondary antibody (Bioster, Wuhan, China), visualized with DAB (Bioster), and counterstained with hematoxylin for 2 min, then dehydrated and mounted.

2.9. Real-Time Quantitative Polymerase Chain Reaction (RT-qPCR). The callus was taken from each group with 4 rats. TRIzol reagent was added to the callus and placed in

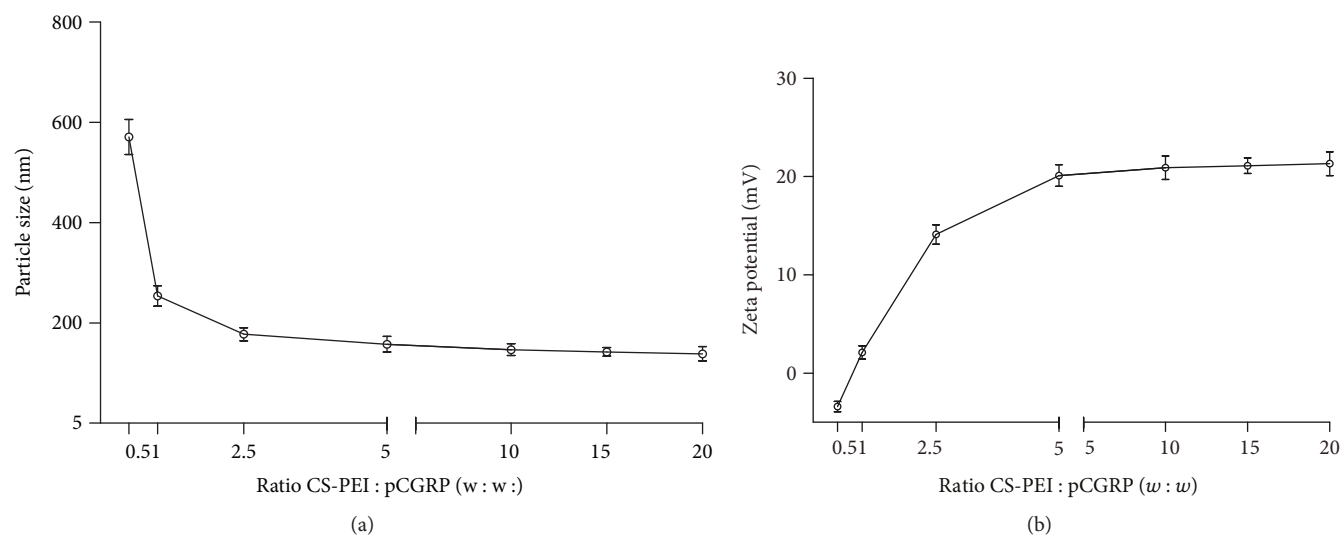


FIGURE 3: Physical properties of CS-PEI/pCGRP with different mass ratios of CS-PEI to pCGRP. (a) Particle size and (b) zeta potential of different CS-PEI/pCGRP nanoparticles.

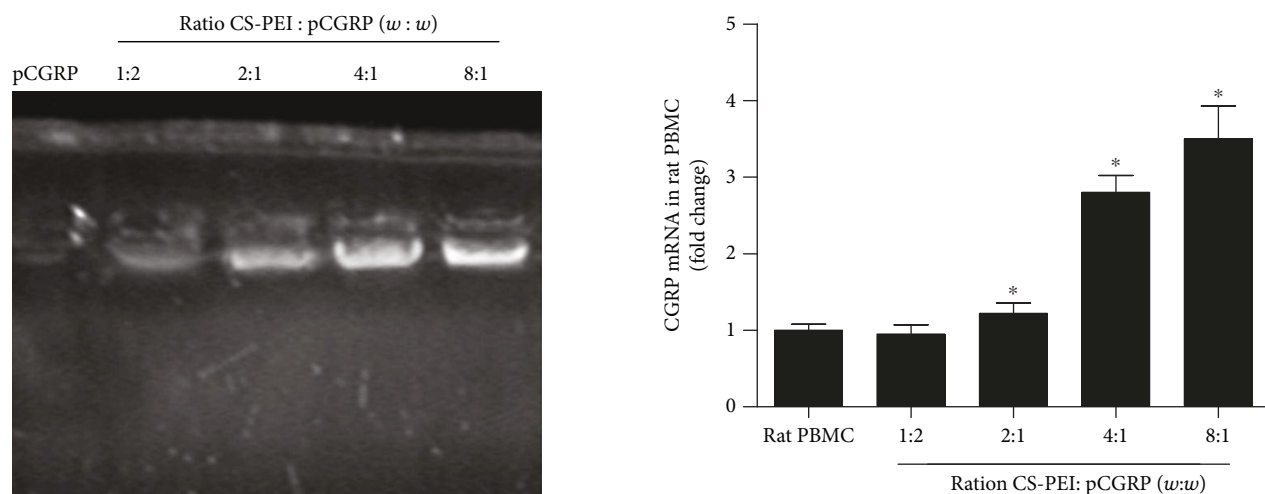


FIGURE 4: DNA binding capacity of CS-PEI in agarose gel retardation assay.

liquid nitrogen. Afterwards, RNA was extracted, and 10 μg of total RNA was quantified by a spectrophotometer (BioPhotometer 6131, Eppendorf) and reverse-transcribed into cDNA. Then, a real-time PCR instrument (Light Cycler,

FIGURE 5: CGRP mRNA expression in rat bone marrow stromal cells (BMSCs) transfected with CS-PEI/pCGRP at different CS-PEI : pCGRP ratios (w : w :). Data are mean \pm standard deviation ($n = 3$). * $P < 0.05$ vs. BMSCs.

Roche) was used to detect the relative expression of ALP, RUNX2, and CGRP, and β -actin was used as a reference gene for PCR reaction. The reaction conditions of the PCR were set to 95°C for 30 sec, then 40 cycles with 60°C for 30 sec and 72°C for 1 min, and finally incubated at 72°C for 1 min and 4°C for extension. Primer synthesis was provided by Guangzhou Funeng Gene Co. Ltd. (Guangzhou, China). The specific primer sequences were shown in Table 1. The results were analyzed using the $2^{-\Delta\Delta\text{Ct}}$ data method. The same procedure was used to detect the CGRP mRNA levels in CS-PEI/pCGRP-transfected BMSCs.

2.10. Western Blot. The total bone protein was extracted from 0.5 g frozen callus, and the total protein was adjusted to the same concentration by the Coomassie Brilliant Blue

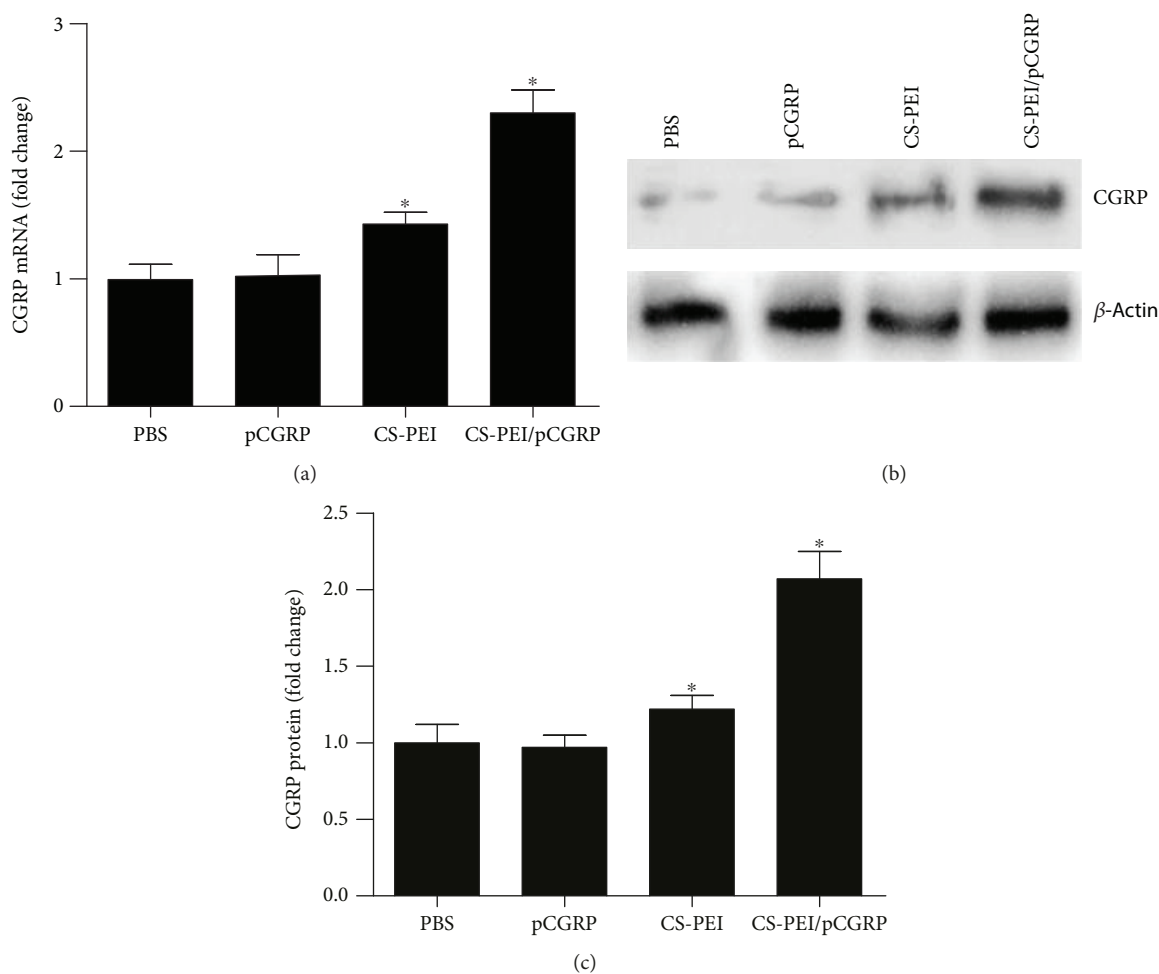


FIGURE 6: CGRP expression in callus of rat femoral fracture model after 3 weeks treatment with CS-PEI/pCGRP. (a) mRNA level of CGRP by RT-qPCR. (b) Representative image of CGRP bands for protein level by western blot. (c) The quantified result of CGRP bands. Data are mean \pm standard deviation ($n = 4$). * $P < 0.05$ vs. the PBS group.

method. The sample was loaded with 50 μ g, electrophoresed on SDS-PAGE, and transferred to PCDF membrane. The electroporated nitrocellulose membrane was blocked with a 50 g/L skim milk blocking solution, after which ALP, RUNX2, CGRP, and β -actin antibodies were added and incubated at 4°C overnight and then incubated with horseradish peroxidase-labeled secondary antibody IgG (Bioستر). Chemiluminescence method was applied for color development and gel quantitative software Quantity One 4.52 was used for analysis. RUNX2, CGRP, and β -actin antibodies were purchased from Bioss Inc., and ALP antibody was purchased from Boster Inc.

2.11. Hematoxylin and Eosin (H&E) Staining. After the rats were sacrificed, the livers were rapidly excised and fixed in 4% paraformaldehyde. Then, the fixed samples were dehydrated, embedded in paraffin, and sectioned to 5 μ m slices. The sections were stained by hematoxylin and eosin for the detection of pathological changes.

2.12. Statistical Analysis. Statistical analysis was performed on SPSS19.0 statistical software. All data were presented

as mean \pm SD, statistically analyzed by a *t*-test and one-way ANOVA. $P < 0.05$ indicated that the difference was significant.

3. Results and Discussion

3.1. The Distribution Degree of PEI on CS-PEI. The initial weight of chitosan was 0.1 g, and the product weight of CS-PEI was 0.135 g, showing the distribution degree of PEI which was 35%. This indicated that the procedure could successfully graft PEI to chitosan.

3.2. $^1\text{H-NMR}$ Analysis and Composition of CS-PEI Nanoparticles. $^1\text{H-NMR}$ spectroscopy was used to investigate the composition of chitosan to PEI. As shown in the CS-PEI spectrum in Figure 2, the signals between 3.3 and 2.8 ppm showed the presence of hydrogen peaks, which was absent in the CS spectrum and was presumed to be the hydrogen peak of PEI. The $^1\text{H-NMR}$ confirms that PEI has been successfully covalently grafted onto chitosan. According to the analysis of peak areas, it could be concluded that one PEI is connected to an average of 29 D-glucosamine units of

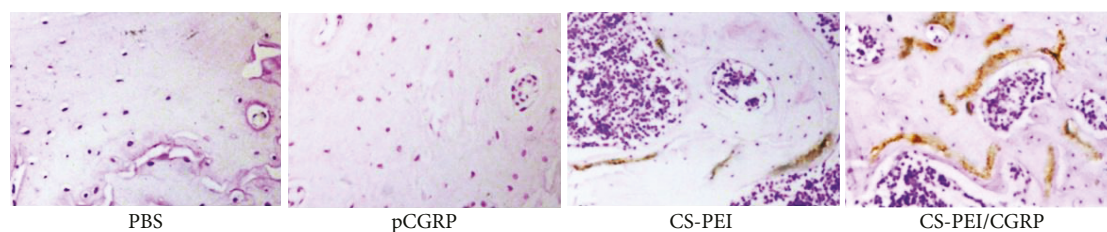


FIGURE 7: CGRP immunohistochemical result in callus of rat femoral fracture model after a 3-week treatment with CS-PEI/pCGRP.

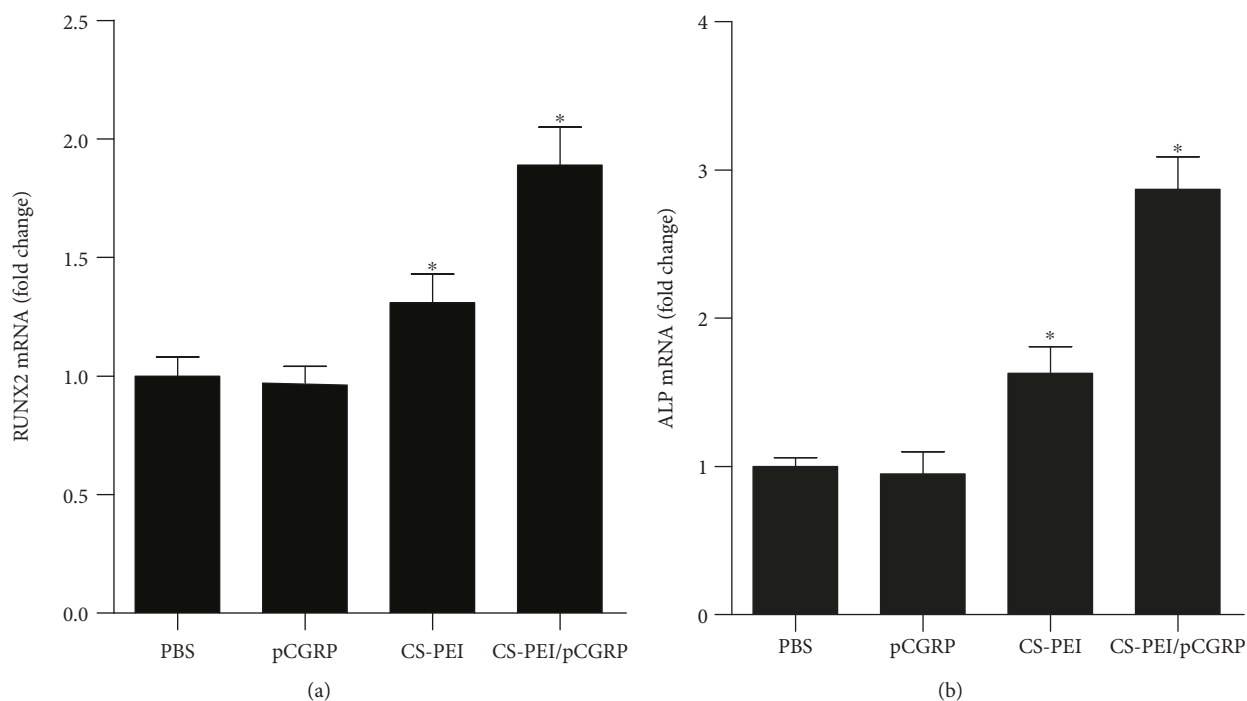


FIGURE 8: RUNX2 and ALP mRNA levels in the callus of rat femoral fracture model after a 3-week treatment with CS-PEI/pCGRP. Data are mean \pm standard deviation ($n = 4$). * $P < 0.05$ vs. the PBS group.

chitosan, which was consistent with the 35% distribution degree calculated by the above dialysis method.

3.3. Size and Potential of CS-PEI/pCGRP Nanoparticles.

Figure 3 showed the particle size and zeta potential of CS-PEI/pCGRP nanoparticles. The results displayed that when the mass ratio was 1:2~1:1, the particle sizes of the nanoparticles were 571.1 ± 34.9 nm and 254.1 ± 20.3 nm (Figure 3(a)), respectively. When the mass ratio was 1:2 to 2.5:1, the zeta potential was increased from -3.4 ± 0.52 mV to 14.1 ± 0.98 mV (Figure 3(b)). With the increase of mass ratio, the particle sizes of composite nanoparticles decreased gradually and the zeta potential gradually increased. When the mass ratio is 5:1, the particle sizes and zeta potentials of CS-PEI/pCGRP nanoparticles tended to be stable and were 157.4 ± 15.6 nm (Figure 3(a)) and 20.1 ± 1.1 mV (Figure 3(b)), respectively. This indicated that the ability compressing DNA was improved as the proportion of CS-PEI polymer in the nanoparticles increased, and the zeta potential of the particles could be effectively increased. The advantage of chitosan is the good degradability and

biocompatibility, and the main drawback is the low efficiency for gene transfection [17]. Studies have shown that the main reason for the low efficiency of chitosan-mediated gene transfection is the lack of buffered amine groups, which leads to the difficulty in escaping from endosomes and lysosomes. Another reason is the strong binding capability of chitosan to DNA, which results in low DNA disassembly and low target gene expression after entry into cells. PEI has a strong ion buffering capacity, which allows DNA to effectively escape the digestion of acidic lysosomes, thus achieving higher transfection efficiency [19, 20]. However, in gene transfection, PEI usually exhibits molecular weight-related cytotoxicity in a dose-dependent manner, mainly due to its significantly positive charge, which leads to strong electrostatic interaction with the cell membrane, resulting in intracellular functional disorder [21]. In addition, PEI is a nondegradable polymer that accumulates in the body and may present an unknown risk for long-term use. Therefore, we selected a relatively low-molecular-weight (1.8 kDa) PEI grafted onto chitosan and tried to produce a gene carrier with low toxicity and high transfection efficiency [20]. It is

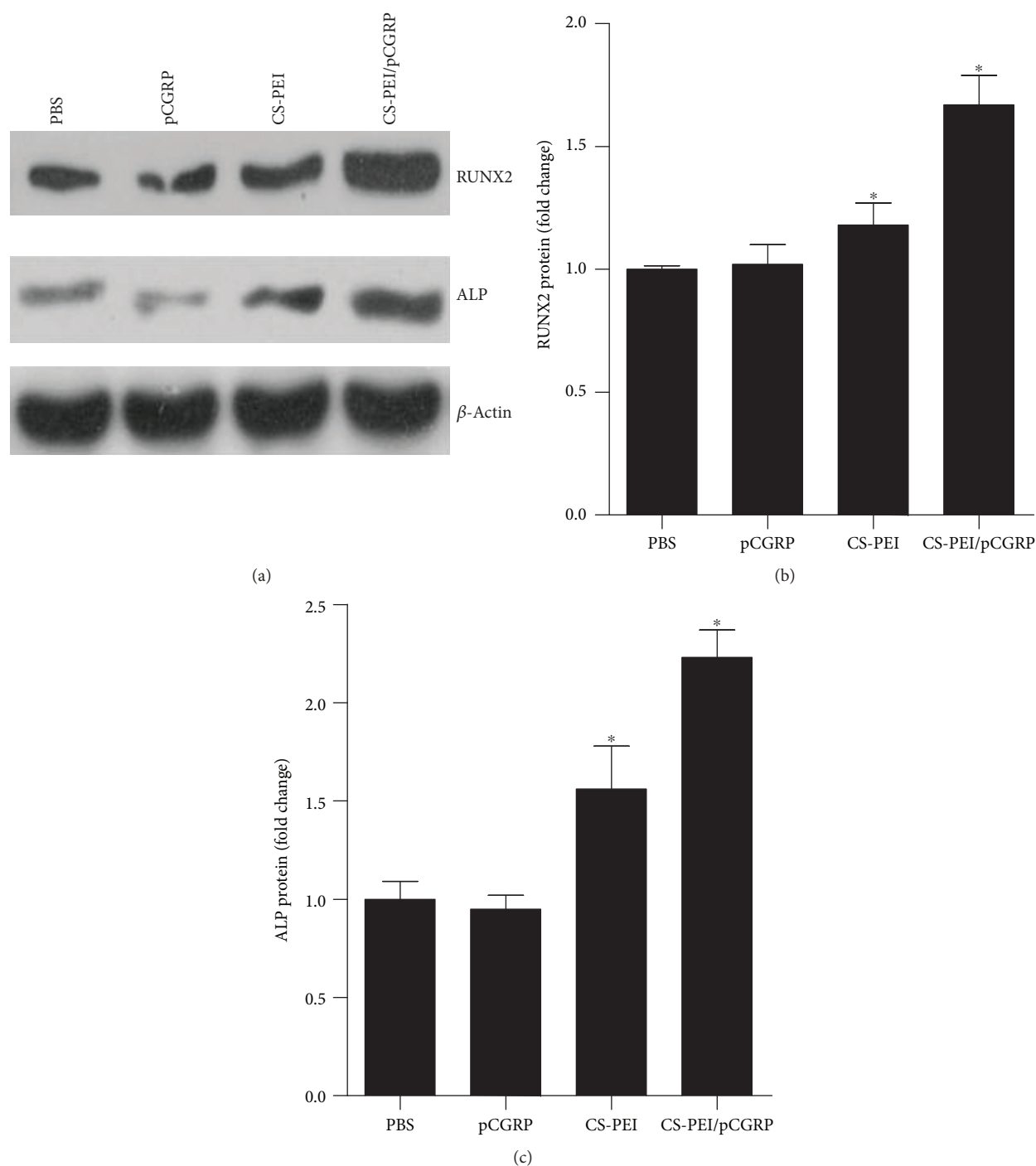


FIGURE 9: RUNX2 and ALP protein levels in callus of rat femoral fracture model after a 3-week treatment with CS-PEI/pCGRP. Data are mean \pm standard deviation ($n = 4$). * $P < 0.05$ vs. the PBS group.

generally believed that a diameter < 200 nm [14, 15] with positive potential is most beneficial for transfection. We found that the mass ratio of CS-PEI:pCGRP affected the particle size and zeta potential. When the mass ratio was higher than 5:1, the CS-PEI/pCGRP nanoparticles had a particle size of less than 200 nm.

3.4. Stability of CS-PEI/pCGRP Nanoparticles. To further determine the loading and protection capability of CS-PEI

on pCGRP, we performed an agarose gel retardation assay. It could be observed from Figure 4 that when the mass ratio of CS-PEI copolymer to pCGRP was less than 2:1, some DNA bands appeared. When the mass ratio reached 4:1, no obvious DNA bands ran out, indicating that the CS-PEI copolymer could fully bind to the pCGRP plasmid when $w:w$ is higher than 4:1. The DNA plasmid is easily degraded by nucleases in the body. In the experiment, DNase I was used to represent the nuclease in the cells. The results

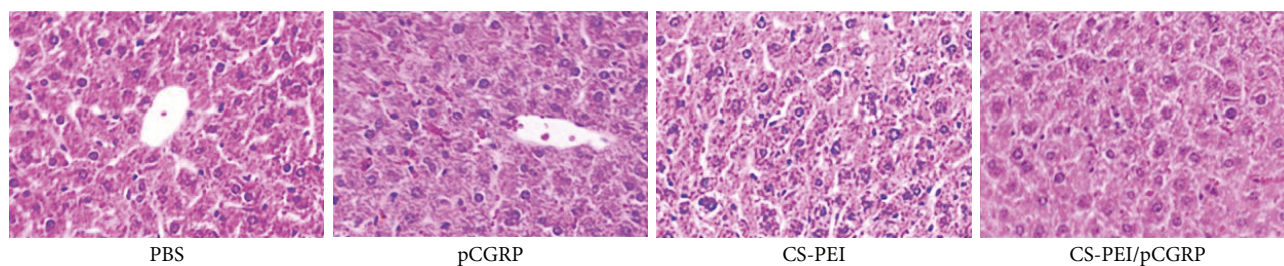


FIGURE 10: The histological section of rat liver after 3 weeks with different treatments of pCGRP, CS-PEI, or CS-PEI/pCGRP.

demonstrated that the antinuclease effect of CS-PEI on the pCGRP plasmid could effectively encapsulate and protect the gene from nuclease degradation. This advantage of CS-PEI would significantly contribute to the improvement of transfection efficiency.

3.5. CS-PEI/pCGRP Nanoparticles Enhance the *In Vitro* Expression of CGRP mRNA in Rat BMSCs. Figure 5 showed the CGRP mRNA levels in BMSCs transfected with CS-PEI/pCGRP. The CGRP mRNA levels increased with increasing of CS-PEI : pCGRP ratio ($w:w$). The level initially increased at the ratio of 2 : 1 and obviously increased from 4 : 1 to 8 : 1. It could be explained by the increased protective ability of CS-PEI.

3.6. CS-PEI/pCGRP Upregulates the Expression of CGRP and Its Downstream Genes in Early Stage of Fracture. In the early healing of fracture (3 weeks), there were no signs of non-healing in the fracture site of rats in the 4 groups. The PBS control group and the pCGRP treatment group had less callus, the fracture line was clear, and the trabecular bone formation was less; the CS-PEI treatment group and the CS-PEI/pCGRP treatment group had more callus, the fracture line was blurred, and the trabecular bone generation was more. The CS-PEI/pCGRP treatment group had more quantities of callus and trabecular bone when compared with the CS-PEI treatment group. The mRNA and protein levels of CGRP in the callus site of rats were detected. It was found that the mRNA and protein expression levels of CGRP were the highest in CS-PEI/pCGRP treatment group, and the mRNA and protein levels of CGRP in the CS-PEI-treated group were increased in a certain level (Figure 6). Further IHC staining detection (Figure 7) showed that the expression of CGRP was the highest in the CS-PEI/pCGRP treatment group, and CGRP was mainly deposited on functionally active osteoblasts around the trabecular bone. These results indicated that CS-PEI had certain repair ability. After CS-PEI polymer delivery, pCGRP could be transfected into the cells of the fracture site to induce more obvious repair effect. Further, by RT-qPCR and western blot studies, it was found that the mRNA of osteogenesis molecules RUNX2 and ALP (Figure 8) and their protein expression levels (Figure 9) were also significantly increased after *in vivo* transfection of pCGRP. Wang et al. [22] have reported that chitosan has a certain effect on bone repair due to its osteoinductivity and progressive substitution of implants by host bones, which

might explain the upregulated CGRP, RUNX2, and ALP expression in the CS-PEI treatment group. However, pCGRP delivered by a CS-PEI copolymer could further enhance the repair effect.

Furthermore, because of the known toxicity of polymeric cations, the biosafety of CS-PEI and CS-PEI/pCGRP was preliminary detected by investigating the appearance of internal organs and evaluating the histological changes in the liver. As shown in Figure 10, all livers in rats of the CS-PEI or CS-PEI/pCGRP treatment group did not present histological changes. And the appearance of the heart, liver, stomach, and kidney in all treatment groups was similar to that in the control group. This indicated that the dosage of CS-PEI or CS-PEI/pCGRP in this study did not show significant toxicity to rats.

The study found that CGRP levels were significantly elevated in the local fracture site and in the patient's plasma at the time of fracture [23, 24], suggesting that this small peptide was likely to be involved in the process of fracture repair. *In vivo* experiments confirmed that CGRP knockout mice showed more severe bone loss than wild-type mice [25]. *In vitro* experiments had also demonstrated that CGRP could induce osteoblast proliferation and differentiation [26]. ALP (alkaline phosphatase) is an important index for evaluating bone formation and bone turnover. During bone formation, osteoblast activity is enhanced. ALP in osteoblasts produces phosphoric acid by enzymatic action and is deposited in the bone with calcium phosphate. RUNX2 is also a specific osteogenic marker expressed by osteoblasts. It is an important transcription factor that activates and initiates the differentiation of BMSCs into osteoblasts and regulates the maturation of osteoblasts. A number of studies have confirmed that CGRP can increase the transcriptional level and protein level of RUNX2 *in vivo* through Hippo signaling pathway [27] and BMP2 signaling pathway [28], thereby accelerating the differentiation of BMSCs into osteoblasts *in vivo*, resulting in the difference in mineralization osteogenesis at the late stage of the fracture. The results of in this study demonstrated that CS-PEI polymer could not only transfect CGRP plasmid into *in vivo* fracture areas but also preserve the biological role of transfected CGRP plasmid.

4. Conclusion

In summary, this study developed a CS-PEI polymer that could encapsulate the rat CGRP plasmid, which could significantly induce bone differentiation into the osteogenesis and

increase calcium deposition. By upregulating the production of CGRP, CS-PEI/pCGRP nanoparticles might regulate the fracture healing process in the early stage and provide a new therapeutic approach for promoting early rehabilitation of patients with fractures in clinics, preventing delayed healing and nonunion of fractures.

Data Availability

The data used to support the findings of this study are available from the corresponding author upon request.

Ethical Approval

All animal experiments were approved by the Ethical Committee of Qinghai Provincial People's Hospital.

Conflicts of Interest

The authors declare that there are no conflicts of interest regarding the publication of this paper.

References

- [1] O. Ström, F. Borgström, J. A. Kanis et al., "Osteoporosis: burden, health care provision and opportunities in the EU: a report prepared in collaboration with the International Osteoporosis Foundation (IOF) and the European Federation of Pharmaceutical Industry Associations (EFPIA)," *Archives of Osteoporosis*, vol. 6, no. 1-2, pp. 59–155, 2011.
- [2] T. P. van Staa, E. M. Dennison, H. G. Leufkens, and C. Cooper, "Epidemiology of fractures in England and Wales," *Bone*, vol. 29, no. 6, pp. 517–522, 2001.
- [3] US Department of Health and Human Services, *Bone Health and Osteoporosis: a Report of the Surgeon General*. U.S. Department of Health and Human Services, Office of The Surgeon General, Rockville, MD, USA, 2004.
- [4] J. A. Kanis, E. V. McCloskey, H. Johansson et al., "European guidance for the diagnosis and management of osteoporosis in postmenopausal women," *Osteoporosis International*, vol. 24, pp. 23–57, 2013.
- [5] International Osteoporosis Foundation, *The Asian Audit: Epidemiology, Costs and Burden of Osteoporosis in Asia 2009*, IOF, Nyon, 2009.
- [6] T. Sekiguchi, N. Suzuki, N. Fujiwara et al., "Calcitonin in a protochordate, *Ciona intestinalis*—the prototype of the vertebrate calcitonin/calcitonin gene-related peptide superfamily," *The FEBS Journal*, vol. 276, no. 16, pp. 4437–4447, 2009.
- [7] C. V. Vause and P. L. Durham, "CGRP stimulation of iNOS and NO release from trigeminal ganglion glial cells involves mitogen-activated protein kinase pathways," *Journal of Neurochemistry*, vol. 110, no. 3, pp. 811–821, 2009.
- [8] Z. Fang, Q. Yang, W. Xiong et al., "Effect of CGRP-adenoviral vector transduction on the osteoblastic differentiation of rat adipose-derived stem cells," *PLoS One*, vol. 8, no. 8, article e72738, 2013.
- [9] S. Q. Li, S. J. Dong, W. G. Xu et al., "Antibacterial hydrogels," *Advanced Science*, vol. 5, no. 5, article 1700527, 2018.
- [10] Z. H. Tang, C. L. He, H. Y. Tian et al., "Polymeric nanostructured materials for biomedical applications," *Progress in Polymer Science*, vol. 60, pp. 86–128, 2016.
- [11] R. J. Mumper, J. Wang, J. M. Claspell, and A. P. Rolland, "Novel polymeric condensing carriers for gene delivery," *Proceedings of the Controlled Release Society*, vol. 22, pp. 178–179, 1995.
- [12] M. Köping-Höggård, I. Tubulekas, H. Guan et al., "Chitosan as a nonviral gene delivery system. Structure-property relationships and characteristics compared with polyethylenimine in vitro and after lung administration in vivo," *Gene Therapy*, vol. 8, no. 14, pp. 1108–1121, 2001.
- [13] S. P. Strand, S. Lelu, N. K. Reitan, C. de Lange Davies, P. Artursson, and K. M. Vårum, "Molecular design of chitosan gene delivery systems with an optimized balance between polyplex stability and polyplex unpacking," *Biomaterials*, vol. 31, no. 5, pp. 975–987, 2010.
- [14] K. Corsi, F. Chellat, L. Yahia, and J. C. Fernandes, "Mesenchymal stem cells, MG63 and HEK293 transfection using chitosan-DNA nanoparticles," *Biomaterials*, vol. 24, no. 7, pp. 1255–1264, 2003.
- [15] S. Mao, W. Sun, and T. Kissel, "Chitosan-based formulations for delivery of DNA and siRNA," *Advanced Drug Delivery Reviews*, vol. 62, no. 1, pp. 12–27, 2010.
- [16] Y. K. Wang, X. Yu, D. M. Cohen et al., "Bone morphogenetic protein-2-induced signaling and osteogenesis is regulated by cell shape, RhoA/ROCK, and cytoskeletal tension," *Stem Cells and Development*, vol. 21, no. 7, pp. 1176–1186, 2012.
- [17] S. K. Tripathi, R. Goyal, P. Kumar, and K. C. Gupta, "Linear polyethylenimine-graft-chitosan copolymers as efficient DNA/siRNA delivery vectors in vitro and in vivo," *Nanomedicine*, vol. 8, no. 3, pp. 337–345, 2012.
- [18] A. Gazdhar, N. Susuri, K. Hostettler et al., "HGF expressing stem cells in usual interstitial pneumonia originate from the bone marrow and are antifibrotic," *PLoS One*, vol. 8, no. 6, article e65453, 2013.
- [19] Y. C. Li, H. Y. Tian, J. X. Ding et al., "Guanidinated thiourea-decorated polyethylenimines for enhanced membrane penetration and efficient siRNA delivery," *Advanced Healthcare Materials*, vol. 4, no. 9, pp. 1369–1375, 2015.
- [20] J.-Q. Gao, Q.-Q. Zhao, T.-F. Lv et al., "Gene-carried chitosan-linked-PEI induced high gene transfection efficiency with low toxicity and significant tumor-suppressive activity," *International Journal of Pharmaceutics*, vol. 387, no. 1-2, pp. 286–294, 2010.
- [21] V. Uskoković and D. P. Uskoković, "Nanosized hydroxyapatite and other calcium phosphates: chemistry of formation and application as drug and gene delivery agents," *Journal of Biomedical Materials Research. Part B, Applied Biomaterials*, vol. 96, no. 1, pp. 152–191, 2011.
- [22] X. Wang, J. Ma, Y. Wang, and B. He, "Bone repair in radii and tibias of rabbits with phosphorylated chitosan reinforced calcium phosphate cements," *Biomaterials*, vol. 23, no. 21, pp. 4167–4176, 2002.
- [23] J. Li, A. Kreicbergs, J. Bergström, A. Stark, and M. Ahmed, "Site-specific CGRP innervation coincides with bone formation during fracture healing and modeling: a study in rat angulated tibia," *Journal of Orthopaedic Research*, vol. 25, no. 9, pp. 1204–1212, 2007.
- [24] G. N. Onuoha, "Circulating sensory peptide levels within 24 h of human bone fracture," *Peptides*, vol. 22, no. 7, pp. 1107–1110, 2001.
- [25] A. K. Huebner, T. Schinke, M. Priemel et al., "Calcitonin deficiency in mice progressively results in high bone turnover,"

- Journal of Bone and Mineral Research*, vol. 21, no. 12, pp. 1924–1934, 2006.
- [26] G. Tian, G. Zhang, and Y. H. Tan, “Calcitonin gene-related peptide stimulates BMP-2 expression and the differentiation of human osteoblast-like cells in vitro,” *Acta Pharmacologica Sinica*, vol. 34, no. 11, pp. 1467–1474, 2013.
- [27] W. Fei, Z. Huiyu, D. Yuxin, L. Shiting, Z. Gang, and T. Yinghui, “Calcitonin gene-related peptide-induced osteogenic differentiation of mouse bone marrow stromal cells through Hippo pathway in vitro,” *Hua Xi Kou Qiang Yi Xue Za Zhi*, vol. 34, no. 3, pp. 286–290, 2016.
- [28] C. Tuzmen and P. G. Campbell, “Crosstalk between neuropeptides SP and CGRP in regulation of BMP2-induced bone differentiation,” *Connective Tissue Research*, vol. 59, Supplement 1, pp. 81–90, 2018.



Hindawi
Submit your manuscripts at
www.hindawi.com

